

UNITU-THEP-006/2001  
CERN-TH/2001-042

## Quantum diffusion of magnetic fields in a numerical worldline approach

Holger Gies<sup>a,b,\*</sup> and Kurt Langfeld<sup>b</sup>

<sup>a</sup> Theory Division, CERN, CH-1211 Geneva 23, Switzerland

and

<sup>b</sup> Institut für Theoretische Physik, Universität Tübingen  
D-72076 Tübingen, Germany

February 2001

### Abstract

We propose a numerical technique for calculating effective actions of electromagnetic backgrounds based on the worldline formalism. As a conceptually simple example, we consider scalar electrodynamics in three dimensions to one-loop order. Beyond the constant-magnetic-field case, serving as a benchmark test, we analyze the effective action of a step-function-like magnetic field – a configuration that is inaccessible to derivative expansions. We observe magnetic-field diffusion, i.e., nonvanishing magnetic action density at space points near the magnetic step where the classical field vanishes.

---

\* Emmy Noether fellow

PACS: 12.20.-m, 11.15.Ha

keywords: worldline, effective action, Monte-Carlo simulation

# Introduction

The worldline formalism was invented by Feynman [1] simultaneously with modern relativistic second-quantized QED, but for a long time it was used only occasionally for actual calculations. Eventually, the observation of a close relation between the worldline formalism and the infinite-string-tension limit of string path integrals triggered further developments of the worldline formalism for QCD [2] and QED [3], particularly for gauge particle amplitudes. Certain computational advantages of this formalism were subsequently recognized and led to numerous applications. Among them, the progress achieved for QED amplitudes with all-order couplings to an external background field is particularly remarkable [4, 5, 6]. The formalism works most elegantly for constant electromagnetic background fields and can be extended to a derivative expansion in the electromagnetic background [7, 8]. For a comprehensive review of the worldline formalism in QED and beyond, see [9].

In the present work, we intend to demonstrate that the worldline formalism is moreover perfectly suited for numerical computations. This is because the path integral over closed loops in spacetime can be approximated by a finite ensemble of loops, which allows for a simple and fast evaluation of expectation values. The latter include observables depending on an *arbitrary* background field.

We illustrate this proposal by means of a simple example: the one-loop effective action of Euclidean scalar QED in three dimensions. The computational task boils down to the calculation of the Wilson loop expectation value using a loop ensemble.

As a first step, we verify the method in Sect. 2 by considering the constant-magnetic-field case, which can also be solved analytically. This serves as a benchmark test for the concrete procedure that we propose. In a second step, the numerical method is applied to a magnetic field resembling a step function in one spatial direction (Sect. 3). This idealized field configuration represents the simplest configuration, which is inaccessible to the standard analytical method for inhomogeneous fields: the derivative expansion. As our main result, we observe diffusion of the magnetic field: the field takes influence on the region of vanishing background field by inducing a nonzero action density therein.

Our conclusions are summarized in Sect. 4, where possible generalization and the road to further application of worldline numerics are sketched.

# 1 The worldline approach to functional determinants

## 1.1 Setup

Our starting point is the unrenormalized Euclidean one-loop effective action of scalar QED in  $D$  dimensions in worldline representation [9], corresponding to the determinant of the gauge-covariant Klein–Gordon operator

$$\Gamma^1[A] = \int_{1/\Lambda^2}^{\infty} \frac{dT}{T} e^{-m^2 T} \mathcal{N} \int_{x(T)=x(0)} \mathcal{D}x(\tau) e^{-\int_0^T d\tau \left( \frac{\dot{x}^2}{4} + ie \dot{x} \cdot A(x(\tau)) \right)}, \quad (1)$$

where the superscript “1” indicates the one-loop level<sup>1</sup>; a gauge-invariant UV regularization at a scale  $\Lambda$  has been performed at the lower bound of the  $T$  integral for the sake of definiteness. In Eq. (1), we encounter a path integral over closed loops in spacetime. Note that there are no other constraints to the loops except differentiability and closeness; in particular, they can be arbitrarily self-intersecting and knotty. The normalization can be determined from the zero-field limit,

$$\mathcal{N} \int \mathcal{D}x(\tau) e^{-\int_0^T d\tau \frac{\dot{x}^2}{4}} \stackrel{!}{=} \text{Tr} e^{\partial^2 T} = \int \frac{d^D p}{(2\pi)^D} e^{-p^2 T} = \frac{1}{(4\pi T)^{D/2}}. \quad (2)$$

Solving Eq. (2) for  $\mathcal{N}$  and inserting this into Eq. (1) leads us to the compact formula

$$\Gamma^1[A] = \frac{1}{(4\pi)^{D/2}} \int d^D x_0 \int_{1/\Lambda^2}^{\infty} \frac{dT}{T^{(D/2)+1}} e^{-m^2 T} \langle W[A] \rangle_x. \quad (3)$$

Here we have split off the integral over the zero-modes of the path integral,  $\int d^D x_0$ , where  $x_0$ , the so-called loop center of mass, corresponds to the average position of the loop:  $x_0^\mu := (1/T) \int_0^T d\tau x^\mu(\tau)$ . In Eq. (3), we introduced the Wilson loop

$$W[A(x)] = e^{-ie \int_0^T d\tau \dot{x}(\tau) \cdot A(x(\tau))} \equiv e^{-ie \oint dx \cdot A(x)}, \quad (4)$$

---

<sup>1</sup>In an abuse of nomenclature, we call the one-loop contribution to the total effective action also “effective action” in the following. The reader should always keep in mind that the Maxwell term (and all higher-order terms) must be added.

and  $\langle(\dots)\rangle_x$  denotes the expectation value of  $(\dots)$  evaluated over an ensemble of  $x$  loops; the loops are centered upon a common average position  $x_0$  (“center of mass”) and are distributed according to the Gaussian weight  $\exp[-\int_0^T d\tau \frac{\dot{x}^2}{4}]$ .

The following  $\tau$ -integral substitution,  $\tau =: Tt$ , is of crucial importance for the numerical realization of the path integral; it suggests introducing *unit loops*  $y$ ,

$$y(t) := \frac{1}{\sqrt{T}} x(Tt), \quad t \in [0, 1], \quad (5)$$

which are parameterized with a unit proptime  $t$ . The remaining integrals can be rewritten accordingly:

$$\int_0^T d\tau \frac{\dot{x}^2(\tau)}{4} = \int_0^1 dt \frac{\dot{y}^2(t)}{4}, \quad \int_0^T d\tau \dot{x}(\tau) \cdot A(x(\tau)) = \int_0^1 dt \dot{y}(t) \cdot [\sqrt{T}A(\sqrt{T}y(t))]. \quad (6)$$

The important advantage is constituted by the fact that the expectation value of  $W[A]$  can now be evaluated over the unit-loop ensemble  $y$ ,

$$\langle W[A(x)] \rangle_x \equiv \langle W[\sqrt{T}A(\sqrt{T}y)] \rangle_y, \quad (7)$$

where the exterior  $T$ -proptime dependence occurs only as a scaling factor of the gauge field and its argument. In other words, while approximating the loop path integral by a finite ensemble of loops, it suffices to have one single unit-loop ensemble at our disposal; we do not have to generate a new loop ensemble whenever we go over to a new value of  $T$ .

Inserting Eq. (7) into Eq. (3), we arrive at the final formula (dropping the subscript of  $x_0$ ):

$$\Gamma^1[A] = \frac{1}{(4\pi)^{D/2}} \int d^D x \int_{1/\Lambda^2}^{\infty} \frac{dT}{T^{(D/2)+1}} e^{-m^2 T} \left\langle W[\sqrt{T}A(\sqrt{T}y)] \right\rangle_y + \text{c.t.}, \quad (8)$$

where we have formally added counter-terms (c.t.) which correspond to a renormalization of the physical parameters. The details of the c.t.’s depend on the dimension, but not on the type of the background field, and will be discussed in the following.

## 1.2 Renormalization

For an accurate evaluation of the effective action of Eq. (8), an *analytic* calculation of the counter-terms is inevitable in order to obtain accurate results by the *numerical* procedure. In the following, we will confine ourselves to the important cases of  $D = 3$  and  $D = 4$  dimensions at the one-loop level.

Let us first discuss the analytical treatment: while for  $D = 3$  the effective action is rendered finite by dropping a field-independent constant, the complete effective action in the 4-dimensional case is renormalized in such a way that the quadratic term in the field strength is given by

$$\Gamma_{\text{quadr.}} = \frac{1}{4g_R^2} \int d^4x F_{\mu\nu}(x) F_{\mu\nu}(x), \quad (9)$$

where  $F_{\mu\nu}(x)$  is the field strength tensor, and  $g_R$  represents the renormalized coupling. In practice, this is done by subtracting the (infinite) quadratic term of the one-loop contribution  $\Gamma^1$  and absorbing it into the bare Maxwell term.

These UV divergencies of the effective action emerge from the lower bound of the proptime integral in Eq. (8), i.e.,  $T \rightarrow 0$ . For small values of the proptime, the Wilson loop expectation value can be calculated exactly (e.g., using heat-kernel techniques):

$$\left\langle W[\sqrt{T}A(\sqrt{T}y)] \right\rangle_y = 1 - \frac{1}{12} T^2 F_{\mu\nu}[A](x) F_{\mu\nu}[A](x) + \mathcal{O}(T^4), \quad (10)$$

where  $x$  is the loop center of mass. The key observation is that, even for  $D = 4$ , the terms of order  $T^4$  are UV-finite upon the proptime integration in Eq. (8). Hence, the completely renormalized effective action, which is suitable for numerical simulations, is

$$\begin{aligned} \Gamma^1[A] = & \frac{1}{(4\pi)^{D/2}} \int d^Dx \int_0^\infty \frac{dT}{T^{(D/2)+1}} e^{-m^2T} \left[ \left\langle W[\sqrt{T}A(\sqrt{T}y)] - 1 \right\rangle_y \right. \\ & \left. + \frac{1}{12} T^2 F_{\mu\nu}[A](x) F_{\mu\nu}[A](x) \right] \\ & + c_D \int d^Dx F_{\mu\nu}[A](x) F_{\mu\nu}[A](x), \end{aligned} \quad (11)$$

where

$$c_3 = -\frac{1}{96\pi} \frac{1}{m} + \mathcal{O}(1/\Lambda), \quad c_4 = -\frac{1}{12} \frac{1}{16\pi^2} \left( \ln \frac{\Lambda^2}{m^2} - C \right) + \mathcal{O}(m^2/\Lambda^2). \quad (12)$$

Here  $\Lambda$  denotes the UV cutoff, and  $C$  is Euler's number. In the  $D = 4$  case, the term  $\sim c_4$  will be absorbed into the bare Maxwell term, defining the running of the coupling, and the cutoff can subsequently be sent to infinity. In  $D = 3$ , the theory is super-renormalizable and the term  $\sim c_3$  represents only a finite shift of the coupling, introducing no running. In the first two lines of Eq. (11), we have already sent the cutoff  $\Lambda$  to infinity, leaving us with a perfectly finite expression. Note that in the case  $D = 3$ , the term of order  $T^2$  in Eq. (10) corresponds to a singularity  $1/\sqrt{T}$ , which is integrable. Hence, the subtraction of this term from the proper-time integral is not mandatory. However, aiming at worldline numerics, the perfect control over the behavior of the integrand at small proper-time  $T$  is required in order to augment the accuracy of the numerical evaluation of the proper-time integral.

Now, the numerical renormalization is similar in spirit to the analytical one, but is complicated by a further problem: evaluating  $\langle W \rangle$  with the aid of the loop ensemble does not produce the small- $T$  behavior of Eq. (10) *exactly*, but, of course, only within the numerical accuracy. Unfortunately, even the smallest deviation from Eq. (10) will lead to huge errors, if we naively plug such a result into Eq. (12); this is because of the factors of  $T$  in the denominator of the integrand for  $T \rightarrow 0$ .

Our solution to this problem is to fit the numerical result for  $\langle W \rangle$  to a polynomial in  $T$  in the vicinity of  $T = 0$ , employing Eq. (10) as a constraint for the first coefficients. Of course, such a fit is completely justified because of our exact knowledge of  $\langle W \rangle$  for small  $T$ . This fit not only represents the renormalization procedure, solving the UV problems, but also facilitates a more precise estimate of the error bars (see below). Finally, employing this fitting procedure only close to  $T = 0$ , the infrared behavior ( $T \rightarrow \infty$ ) of the integrand remains untouched, and our approach is immediately applicable, also in the case  $m = 0$ .

Both renormalization procedures, the analytical as well as the numerical, generalize straightforwardly to higher dimensions; here, either additional subtractions from the integrand (for the analytical case), or polynomial fits with higher-order constraints (for the numerical case) are required: for example, increasing the dimension by 2 requires one more subtraction/constraint in the small- $T$  behavior of the integrand.

Finally, it should not be concealed that these procedures become increasingly difficult to higher order in perturbation theory for massive theories in  $D \geq 4$ . Then, a mass renormalization is also necessary, requiring careful analyses of the UV behavior of double proper-time integrals [12].

### 1.3 Numerical simulation

Now, the route to the effective action is clear:

- (1) generate a unit loop ensemble distributed according to the weight  $\exp[-\int_0^1 dt y^2/4]$ , e.g., employing the technique of normal (Gaussian) deviates;
- (2) compute the integrand for arbitrary values of  $T$  (and  $x$ ); this involves the evaluation of the Wilson loop expectation value for a given background gauge field;
- (3) perform the renormalization procedure and add the c.t.'s to the integrand;
- (4) integrate over the proptime  $T$  in order to obtain the Lagrangian, and also over  $x$  for the action.

From a general viewpoint, there are two sources of systematical error which are introduced by reducing the degrees of freedom from an infinite to a finite amount: first, the loop path integral has to be approximated by a finite number of loops; second, the proptime  $t$  of each loop has to be discretized. Contrary to this, the spacetime does not require discretization, i.e., the loop ensemble is generated in the continuum.

Of course, the various steps can be carried out using different numerical methods; let us outline our choice of tools in detail. For this purpose, let  $N_l$  denote the number of loops which are used to estimate the Wilson loop expectation value in Eq. (7), and  $n_l$  the number of space points which are employed to specify a particular loop. The points of a particular loop  $y_i, i = 1 \dots n_l$ , are generated by a standard heat bath algorithm, where the boundary conditions  $y_1 = 0, y_{n_l} = 0$  are enforced. After a proper thermalization, all coordinates  $y_i$  are shifted equally in order to implement the center of mass condition  $\langle y_i \rangle = x_0$ . This procedure is then repeated  $N_l$  times to generate the loop ensemble.

Approximating  $\langle W \rangle$  of Eq. (7) by an average over a finite number of loops, the standard deviation provides an estimate of the statistical error. Approximating the loops by the finite number  $n_l$  of space points results in a systematic error that can be estimated by repeating the calculation for several values  $n_l$ . The number  $n_l$  should be chosen large enough to reduce this systematic error to well below the statistical one. It will turn out that the choice  $N_L = 1000$  and  $n_l = 100$  yields results, for the applications below, which are accurate at the per cent level. We stress, however, that  $\approx 20000$  (dummy) heat bath steps are required to properly thermalize the loop ensemble.

## 2 Benchmark test: constant magnetic background field

Since analytic results are available for the case of a constant magnetic background field  $B$ , we will investigate in this section the efficiency of our numerical loop approach to the scalar functional determinant.<sup>2</sup> For simplicity, we consider three Euclidean spacetime dimensions,  $D = 3$ . Up to a field-independent constant, the one-loop effective-action density (Lagrangian)  $\mathcal{L}^1$  for scalar QED in  $D = 3$  is given by [9, 11]

$$\mathcal{L}^1 \equiv \Gamma^1(B)/V_3 = \frac{B^{3/2}}{(4\pi)^{3/2}} g\left(\frac{m^2}{B}\right), \quad (13)$$

where  $V_3$  denotes the volume and

$$g(z) = \int_0^\infty \frac{dT}{\sqrt{T}} I(T, z), \quad I(T, z) = \frac{1}{T^2} \left[ \frac{T}{\sinh T} - 1 \right] \exp\{-zT\}. \quad (14)$$

The exact integrand  $I(T, z)$  in Eq. (14) is compared with our loop estimate in Fig. 1 for the case  $m^2 = 0$ , i.e.,  $z = 0$ . The numerical estimate for  $g(m^2/B)$  is also shown. The agreement between the two curves is satisfactory and the exact results for  $I(T, z)$  as well as for  $g(m^2/B)$  lie well within the error bars produced by the numerics.

As mentioned above, the error bars correspond to the statistical error of the ensemble average. Regarding the quantity  $\langle W \rangle$  with its dependence on  $T$ , the original error bars are rather independent of  $T$ ; but multiplying  $\langle W \rangle$  by a  $T$ -dependent function (cf. Eq. (8)) causes a modulation of the error bars. In particular for  $T \rightarrow 0$ , the  $1/\sqrt{T}$  singularity leads to an unbounded enhancement of the error bars for small  $T$  in the function  $I(T, x)$  (see left panel of Fig. 1). Fortunately, the integrand in this regime is known *exactly* as given in Eq. (10) in the form of an asymptotic series. As mentioned above for the numerical renormalization procedure, this information can be used for a constraint fit of the numerical result to a polynomial in  $T$  around  $T = 0$ , keeping the first terms corresponding to Eq. (10) fixed. Then, the error bars of the ensemble average translate into errors for the higher coefficients of the polynomial. This polynomial is then matched to the pure numerical result at that value of  $T$  where the error bars of the two results are comparable. The final result is visible on the left panel of Fig. 1.

---

<sup>2</sup>Incidentally, another exactly solvable system is known [10] with a background field resembling a solitonic profile in one dimension.



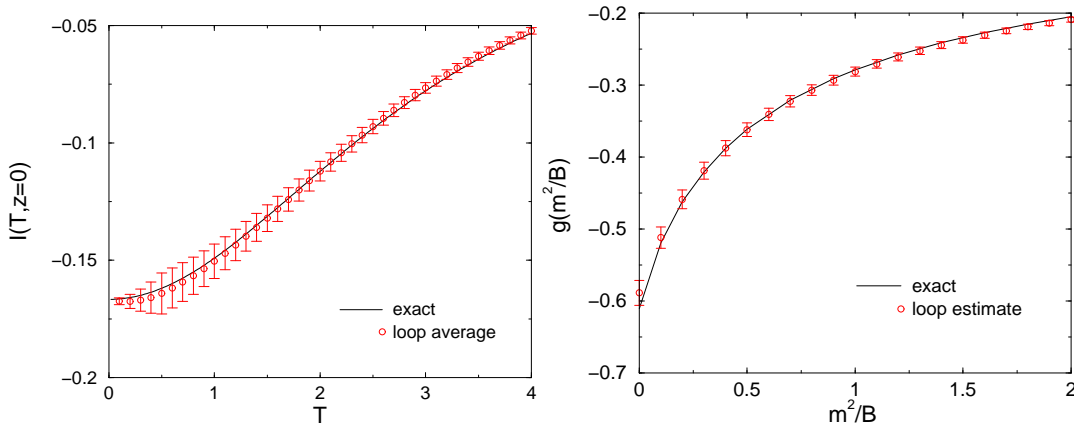


Figure 1: Proptime integrand  $I(T, z = 0)$  (left panel) and integral  $g(m^2/B)$  (right panel) of the one-loop effective action for the case of a constant magnetic background field. The analytically known exact results (solid lines) are compared with the numerical findings (circles with error bars).

It should be noted, that the error bars in Fig. 1 (and the following figures) are highly correlated from point to point, since the same loop ensemble has been used for the evaluation of each point. This correlation can, of course, easily be reduced by updating the loop ensemble with a few heat bath steps inbetween at the expense of computational time.

### 3 Magnetic-field diffusion

In this section, we study the one-loop effective action of Eq. (11) for the case of a magnetic background field, resembling a step function in space. In particular, we consider a time-like constant background field  $B$ , i.e., a field which is independent of the third coordinate called Euclidean time. We choose the  $B$  field, being a (pseudo-)scalar over the spatial  $xy$  plane, as

$$B(x, y) = -\theta(x) B_0, \quad \vec{A}(x, y) = \theta(x) \frac{1}{2} (y, -x) B_0, \quad (15)$$

where  $\theta(x)$  is the step function, i.e.,

$$\theta(x) = 1, \quad \forall x \geq 0, \quad \theta(x) = 0, \quad \forall x < 0.$$

Note that because of the sudden variation of the background field at the step, the effective action cannot be obtained within a derivative expansion. By contrast, such a discontinuity represents no obstacle for the numerical

worldline approach proposed in this work. Discontinuities do not induce (artificial) singularities, but are smoothly controlled by the properties of the loop ensemble. This ensemble resembles a cloud, exhibiting finite extension and slowly varying density, and being centered at some particular spacetime point  $x_0$  which is the center of mass of each loop in the cloud. While running with this  $x_0$  towards and across the step, that part of the volume of the loop cloud which “feels” the magnetic field increases smoothly; therefore, the effective-action density (effective Lagrangian)  $\mathcal{L}^1$ , being the proptime integrated information of what the loop cloud measures, will be smooth, too.

In order to numerically evaluate the effective action for the case of Eq. (15), we employ the loop approach outlined in the previous section. This approach provides for statistical error bars which allow to estimate whether the number of loop ensembles is large enough. In order to study the systematic errors, such as the limited number of spacetime points  $n_l$  specifying a loop and the limited number  $n_T$  of thermalization sweeps, we shall employ three sets of loop ensembles (see Table 1). Defining

$$g\left(\frac{m^2}{B_0^2}, xB_0^{1/2}\right) := \frac{(4\pi)^{3/2}}{B_0^{3/2}} \mathcal{L}^1(\vec{x} = (x, 0, 0)) \quad (16)$$

in analogy to Eq. (13), the final numerical result for the effective action is shown in Fig. 2, left panel. As expected, the effective-action density is nonzero even in the region  $x < 0$  where the background field  $B(\vec{x})$  vanishes. For increasing mass, the contributions from large proptime  $T$  are exponentially suppressed in the integrand. Since the proptime controls the size of the loop cloud, the large loop clouds contribute less to the action density when the mass is large. Hence, the effective-action density for an increasing mass becomes reduced. (From an alternative viewpoint, the limit of large mass and small field are identical for dimensional reasons.)

We find that the effective action decreases exponentially in the “forbidden” region, which is depicted in Fig. 2, right panel; here we defined the

Table 1: Simulation parameters

	$n_l$	$n_T$
set A	100	150000
set B	75	50000
set C	50	50000

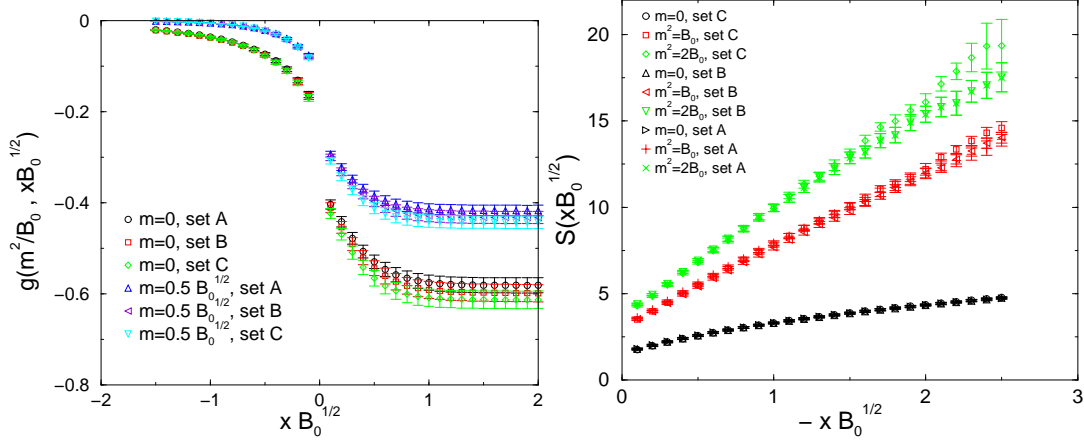


Figure 2: Effective-action density in the vicinity of the magnetic step ( $x = 0$ ). On the left panel, the diffusion profile is visualized. The logarithmic plot on the right panel reveals the exponential nature of the diffusion depth.

quantity

$$-g\left(\frac{m^2}{B_0}, xB_0^{1/2}\right) =: \exp\left[-S\left(xB_0^{1/2}\right)\right], \quad (17)$$

and plotted  $S(xB_0^{1/2})$  for several values of the scalar mass  $m$ . This phenomenon of obtaining a nonzero effective-action density even in a region where the background field vanishes may be called *quantum diffusion* of the magnetic field.

Large values of  $S$  imply that the effective-action density  $\sim g\left(m^2/B_0, xB_0^{1/2}\right)$  is small due to cancellations. In this case, a sufficiently large number of loop points  $n_l$  and of thermalization sweeps is requested. The results indicate that the function  $S(xB_0^{1/2})$  can be fitted for  $x\sqrt{B_0}$  by the ansatz

$$S(y) = \alpha + \beta y, \quad y = xB_0^{1/2}, \quad (18)$$

where the quantities  $\alpha$  and  $\beta$  depend on  $m^2/B_0$ . The diffusion depth  $l$  of the magnetic field can be defined as the inverse of  $\beta$ , i.e.,  $l = 1/(\beta\sqrt{B_0})$ . An estimate of this parameter has been plotted versus the mass  $m$  in Fig. 3. As expected, the diffusion coefficient  $\beta$  rises with increasing mass scale  $m$ . The function

$$\beta(m^2/B_0) = 0.7627 + 3.255 \left(\frac{m^2}{B_0}\right)^{1/2} \quad (19)$$

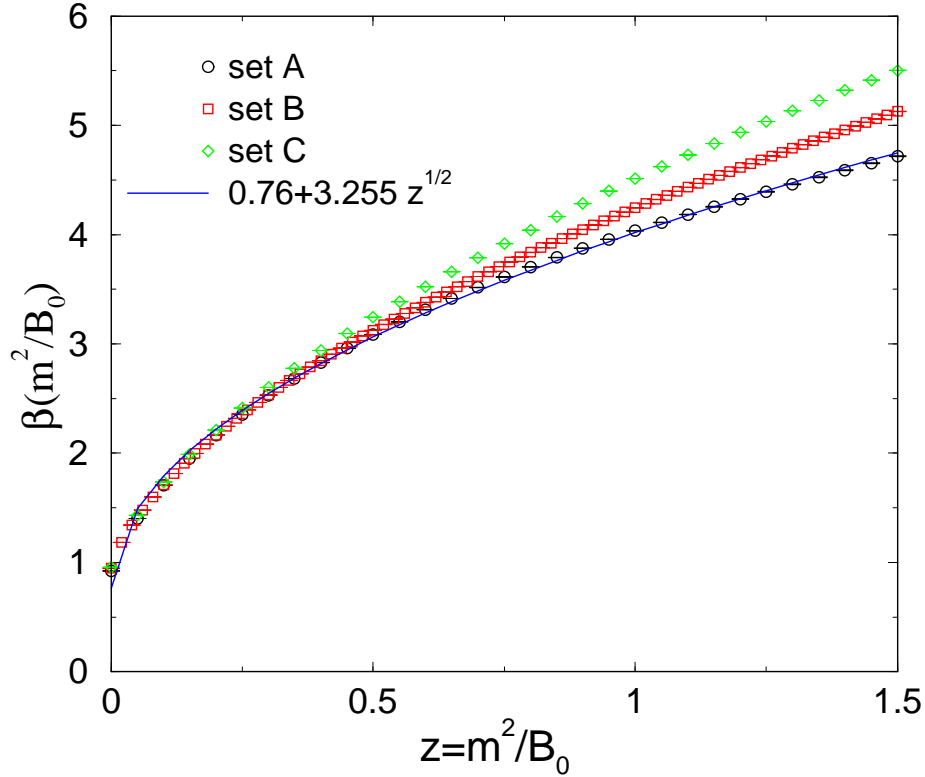


Figure 3: Inverse diffusion depth  $\beta$  versus mass-to-magnetic-field ratio. The plot symbols depict the numerical results, whereas the solid line represents the fit of Eq. (19) adjusted to the optimized loop ensemble A.

nicely fits the high quality numerical data set A (see figure 3).

In order to get an understanding of these numbers, let us perform the following heuristic consideration: at a first glance, one might expect that the magnetic diffusion obeys the simple law  $\sim e^{-\text{const.}\cdot mx}$ , since the mass seems to be the only scale in the field-free region of space; this would correspond to  $\beta = \text{const.} \cdot (m^2/B_0)^{0.5}$ . However, if this simple law were true, the massless limit  $m = 0$  would be obscure, since then the magnetic field would diffuse into the field-free region without any damping. Hence, there must be an additional dependence of the exponent on the magnetic field in order to account for a reasonable massless limit. Moreover, the mass is indeed not the only scale in the field-free region, because the loop cloud is a nonlocal object that always “feels” the strength of the magnetic field. In fact, it is the constant first term in  $\beta$  in Eq. (19) that exactly accounts for this dependence of the magnetic diffusion on the strength of the magnetic field. Only for larger masses (or weaker fields),  $m^2 \simeq B_0/4$ , the intuitively expected diffusion law

of the form  $\sim e^{-\text{const.}\cdot mx}$  begins to dominate; in this regime, we find

$$l \approx 0.31/m . \quad (20)$$

In the present work, the precision of the numerics for the action density in the field-free region restricts the investigation to mass values of  $m^2 < 1.5B_0$ ; beyond this, the strong exponential decrease beyond the step prohibits a reliable analysis of the diffusion depth.

## 4 Conclusion and Outlook

Beyond any particular result of the present work, we would like to remark in the first place that our approach to the worldline formula (see Eq. (8)) for the one-loop effective action offers a vivid picture of the quantum world. Consider a spacetime point  $x$  at a proptime  $T$ ; then, the loop ensemble is centered upon this point  $x$  and resembles a loop cloud with Gaussian “density” and “spread”. Increasing or lowering the proptime  $T$  corresponds to bloating or scaling down the loop cloud or, alternatively, zooming out of or into the microscopic world. The effective-action density at each point  $x$  finally receives contributions from every point of the loop cloud according to its Gaussian weight (times the mass term and other factors) and averaged over the proptime. This gives rise to the inherent nonlocality and nonlinearity of the effective action, because every point  $x$  is influenced by the field of any other point in spacetime experienced by the loop cloud.

In particular, we considered the one-loop contribution to the effective action in scalar electrodynamics in three spacetime dimensions; in the beginning, we were able to reproduce the analytically well-known case of a constant magnetic background field, serving as a testing ground for our numerical procedures including renormalization to one-loop order. Incidentally, the zero-mass limit (or, alternatively, the ultra-strong magnetic field limit) is also covered by our approach without additional difficulties.

We furthermore tackled the problem of a step-function-like magnetic background field, illustrating the stability of our approach also for discontinuous field configurations. For this case, we observed a diffusion of the magnetic field, i.e., nonzero action density even at a distance from the magnetic field. This phenomenon is obviously nonlocal, since an expansion around a point of zero background field gives a zero result to any finite order. But the diffusion phenomenon appears to be also nonperturbative in the same sense as the Schwinger mechanism of pair production [11], at least for not too large values of the mass; this is suggested by the functional form of the diffusion for small mass:  $\exp(-S(xB_0^{1/2})) \sim \exp(-0.7627 \cdot \sqrt{B_0}x)$ ; this result cannot

be expanded in terms of the coupling constant, being rescaled in the field (only an expansion in terms of the square root of the coupling constant is possible).

Perhaps the main advantage of the numerical worldline approach to functional determinants is that no a-priori information, such as certain symmetries of the background field or a suitably chosen set of base functions, has to be exploited; if the loop ensemble has been thermalized properly, any background field can immediately be plugged into the algorithm.

One drawback of the numerical approach lies in the fact that it applies only to Euclidean quantum field theory; this is because the action governing the distribution of the loops must be positive.

The present paper paves the way to further generalizations such as fermionic functional determinants; our approach could facilitate a systematic numerical investigation of these determinants. Results could be compared with several results known from analytical considerations (see, e.g., [13]). Although the treatment of fermions in the worldline formalism can be most elegantly formulated via Grassmann representations (see, e.g., [14]), a numerical approach has to rely on a bosonic representation of the path integrals [1, 15]. In practice, this means that the Dirac algebraic elements in the worldline action are accompanied by a path-ordering prescription. Similar complications occur for nonabelian gauge fields and color-charged fermions or scalars. Whereas such path ordering is difficult to deal with in analytical approaches, a numerical evaluation can immediately take care of such a prescription. This is because the loops are discretized in the proper-time parameter anyway, consisting of  $n_l$  “links”; the path ordering then is nothing but a simple (matrix-)multiplication of these links.

Recently [16], a new approach was designed to improve the still unpleasant situation [17] when lattice QCD is studied at finite baryon densities: the basic idea to circumvent the problems [18] with lattice fermions is a calculation of the *continuum* fermion determinant for arbitrary entries of the gluon field, which subsequently is the subject of a lattice discretization. This program was successfully applied to the case of heavy quarks [16]. The formulation of the present paper stirs the hope that the concept of [16] might be extended to the realistic case of light quarks.

Further possible and straightforward applications can be found in the context of estimating quantum energies to solitonic fields (see [19]), or in the context of thermal field theory or Casimir vacua (for analytical worldline approaches, see, e.g., [20]). The latter cases are connected with a compactification of the Euclidean spacetime manifold; these topological modifications can be imposed directly on the loop ensemble in our approach. For example, compactifying the Euclidean time direction at finite temperature will result

in closed loops that wind several times around the time-like cylinder. Work in these directions is in progress.

Finally, it is obvious that the step-like magnetic field is not physical at all in a strict sense, because such a sharp drop-off cannot be produced by real laboratory magnets; nevertheless, the step-like field can be regarded as a limiting case of a real physical situation, being useful for an estimate of possible effects caused by rapid variations of a magnetic field. For instance, as a matter of principle, magnetic diffusion can be included in the discussion of the Aharonov-Bohm effect: if the propagating particle is no longer considered as a quantum mechanical point particle, but as a quantum field, it will be affected by the quantum diffusion of the solenoid's magnetic field; but a measurable effect can only arise, if the particle's distance from the solenoid is of the order of a few Compton wavelengths.

Beyond that, we would like to mention that our results for the step-like magnetic field are of some significance for the experiments being currently performed at PVLAS (Legnaro) and BMV (Toulouse) [21], in which is measured the optical birefringence of the quantum vacuum exposed to a magnetic field. For example in the PVLAS experiment, the polarization axis of a laser beam is affected by a (6–9 T)-magnetic field with a diameter of 1 m; the magnetic field drops off over a distance of 10 cm, and the question arises as to whether this drop-off will influence the rotation of the polarization axis as predicted by a constant-field QED calculation.

The refractive indices of the modified vacuum are proportional to the energy density induced by the magnetic field (for a review, see [22]). For weak magnetic fields, the energy density is directly related to the (Euclidean) effective-action density. Provided that our present results also hold for  $D = 4$  spinor QED at least qualitatively, we can exclude any further influence of the drop-off region, since the magnetic diffusion in this case ( $m \gg B$ ) occurs at the order of a Compton wavelength  $1/m$ . This “zero-result” is supported by considerations within a derivative expansion, where the natural expansion parameter is given by the Compton wavelength over the length of the field variation (e.g.,  $\simeq 4 \times 10^{-12}$  for the PVLAS). Only the constant-field result integrated over the size of the magnet including the drop-off region need be taken into account.

## Acknowledgement

We would like to thank W. Dittrich for helpful discussions and for carefully reading the manuscript. H.G. gratefully acknowledges insightful discussions with C. Schubert. K.L. is indebted to H. Reinhardt for encouragement and

support. This work has been supported in part by the Deutsche Forschungsgemeinschaft under contract Gi 328/1-1.

## References

- [1] R.P. Feynman, Phys. Rev. **80**, 440 (1950); **84**, 108 (1951).
- [2] Z. Bern and D.A. Kosower, Nucl. Phys. **B362**, 389 (1991); **B379**, 451 (1992).
- [3] M.J. Strassler, Nucl. Phys. **B385**, 145 (1992).
- [4] M. G. Schmidt and C. Schubert, Phys. Lett. **B318**, 438 (1993) [hep-th/9309055].
- [5] R. Shaisultanov, Phys. Lett. **B378**, 354 (1996) [hep-th/9512142].
- [6] M. Reuter, M. G. Schmidt and C. Schubert, Ann. Phys. **259**, 313 (1997) [hep-th/9610191].
- [7] D. Cangemi, E. D'Hoker and G. Dunne, Phys. Rev. D **51**, 2513 (1995) [hep-th/9409113].
- [8] V. P. Gusynin and I. A. Shovkovy, J. Math. Phys. **40**, 5406 (1999) [hep-th/9804143].
- [9] C. Schubert, hep-th/0101036, to appear in Phys. Rep. (2001).
- [10] D. Cangemi, E. D'Hoker and G. Dunne, Phys. Rev. D **52**, 3163 (1995) [hep-th/9506085]; G. Dunne and T. Hall, Phys. Rev. D **58**, 105022 (1998) [hep-th/9807031]; Phys. Lett. **B419**, 322 (1998) [hep-th/9710062].
- [11] J. Schwinger, Phys. Rev. **82**, 664 (1951).
- [12] V. I. Ritus, Sov. Phys. JETP **42**, 774 (1975); W. Dittrich and M. Reuter, Springer Lect. Notes Phys. **220**, 1 (1985); D. Fliegner, M. Reuter, M. G. Schmidt and C. Schubert, Theor. Math. Phys. **113**, 1442 (1997) [hep-th/9704194].
- [13] M. P. Fry, Int. J. Mod. Phys. **A12**, 1153 (1997); Phys. Rev. D **62**, 125007 (2000) [hep-th/0010008].



- [14] E. D'Hoker and D. G. Gagne, Nucl. Phys. **B467**, 272 (1996) [hep-th/9508131]; J. W. van Holten, Nucl. Phys. **B457**, 375 (1995) [hep-th/9508136].
- [15] A. O. Barut and I. H. Duru, Phys. Rep. **172**, 1 (1989).
- [16] K. Langfeld and G. Shin, Nucl. Phys. **B572** (2000) 266.
- [17] I. M. Barbour, talk presented at Workshop on QCD at Finite Baryon Density: A Complex System with a Complex Action, Bielefeld, Germany, 1998.
- [18] M. A. Stephanov, Phys. Rev. Lett. **76**, 4472 (1996).
- [19] N. Graham, R. L. Jaffe, M. Quandt and H. Weigel, *Quantum energies of interfaces*, hep-th/0103010;  
E. Farhi, N. Graham, R. L. Jaffe and H. Weigel, Nucl. Phys. **B585** (2000) 443, [hep-th/0003144];  
Phys. Lett.**B475** (2000) 335, [hep-th/9912283].
- [20] D. G. McKeon and A. Rebhan, Phys. Rev. **D 47**, 5487 (1993) [hep-th/9211076]; I. A. Shovkovy, Phys. Lett. **B441**, 313 (1998) [hep-th/9806156]; R. Venugopalan and J. Wirstam, hep-th/0102029.
- [21] E. Zavattini, Proc. of the *QED2000, 2nd Workshop on Frontier Tests of Quantum Electrodynamics and Physics of the Vacuum*, Ed. by D. Amati, G. Cantatore, E. Zavattini, and R.S. Hayano (2001); C. Rizzo, *ibid.* See also the URL of the PVLAS experiment: <http://sunlnl.lnl.infn.it/~pvlas/home.htm>
- [22] W. Dittrich and H. Gies, Springer Tracts Mod. Phys. **166**, 1 (2000).